magnetochemistry

MDPI

Article

1D Chains of Lanthanoid Ions and a Dithienylethene Ligand Showing Slow Relaxation of the Magnetization

Mudasir Ahmad Yatoo [1], Goulven Cosquer [1,2], Masakazu Morimoto [3], Masahiro Irie [3], Brian K. Breedlove [1] and Masahiro Yamashita [1,2,*]

1 Department of Chemistry, Graduate School of Science, Tohoku University, Aramaki-Aza-Aoba, Aoba-ku, Sendai 980-8578, Japan; muda.amu@gmail.com (M.A.Y.); cosquer.g@m.tohoku.ac.jp (G.C.); breedlove@m.tohoku.ac.jp (B.K.B.)

2 Core Research for Evolutional Science and Technology (CREST), Japan Science and Technology (JST), 4-1-8 Kawaguchi, Saitama 332-0012, Japan

3 Department of Chemistry and Research Center for Smart Molecules, Rikkyo University, Nishi-Ikebukuro 3-34-1, Toshima-ku, Tokyo 171-8501, Japan; m-morimoto@rikkyo.ac.jp (M.M.); iriem@rikkyo.ac.jp (M.I.)

* Correspondence: yamasita.m@gmail.com; Tel.: +81-22-765-6547

Academic Editors: Marius Andruh and Liviu F. Chibotaru

Received: 12 February 2016; Accepted: 25 March 2016; Published: 31 March 2016

Abstract: Three isostructural 1D lanthanoid complexes with the general formula $\{[Ln_2(DTE)(H\text{-}DTE)(MeOH)_2]\cdot 2H_2O\}_n$ (Ln = Tb, Dy, and Yb; DTE = 1,2-bis(5-carboxyl-2-methyl-3-thienyl) perfluorocyclopentene) were synthesized. In the 1D chain structure of each complex, lanthanide ions are seven coordinate with a capped trigonal prism geometry. The 1,2-bis(5-carboxyl-2-methyl-3-thienyl) perfluorocyclopentene (DTE) ligand adopts a parallel configuration in these complexes, which results in the loss of the photo-isomerization ability of the ligand. From magnetic measurements, each complex undergoes slow relaxation of the magnetization via multiple processes in a dc field.

Keywords: Lanthanide; slow magnetic relaxation; coordination polymer

1. Introduction

Single-molecule magnets (SMMs) which retain magnetization for long periods of time in the absence of an external magnetic field are being investigated vigorously these days for potential applications in a variety of fields, including molecular spintronics [1,2], data storage devices [3], and quantum computing [4,5]. Lanthanide based SMMs have large single-ion magnetic anisotropies, and the energy splitting of the ground state of lanthanide ions is affected by the crystal field surrounding the ion [6]. Thus, slight modification of the crystal field can generate a significant change in the ground state splitting, which will affect the magnetic anisotropy of the ion and influence the SMM behavior. In other words, the SMM behavior can be tuned by adjusting the crystal field. In order to make a useful device, the tuning must be *in situ*, and several methods, such as photo-irradiation [7], protonation/deprotonation [8] of the complex and isomerism of the ligands [9], have been devised. Isomerization by light irradiation is the easiest method because a wide range of wavelengths can be used and desired isomers can be selectively obtained. 1,2-bis(5-carboxyl-2-methyl-3-thienyl) perfluorocyclopentene (DTE) is a photochromic ligand with two structural isomers: the closed form, which is dominate under ultraviolet (UV) radiation, chiral, and conjugated, and the open form, which occurs under visible radiation, shows only axial chirality, and is non-conjugated (Figure 1) [10]. DTE

can bridge lanthanide ions, and their magnetic properties are affected by switching between the two forms of the ligand.

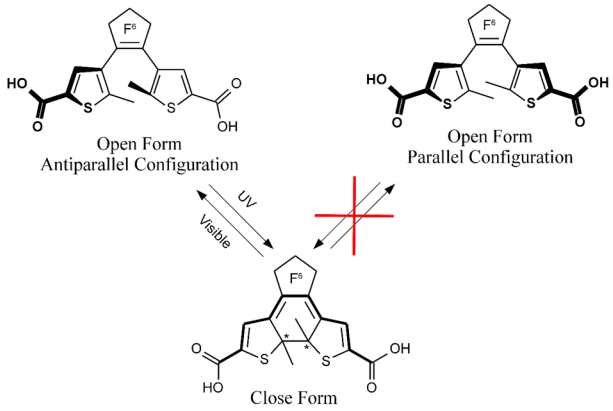

Figure 1. Photochromic 1,2-bis(5-carboxyl-2-methyl-3-thienyl) perfluorocyclopentene (DTE) ligand with two carboxylic groups in the open and closed form. Asymmetric carbon atoms are noted with a * mark.

In this work, we report the synthesis and magnetic properties of 1D chains of lanthanide ions and a DTE ligand with the general formula $\{[Ln_2(DTE)(H\text{-}DTE)(MeOH)_2]\cdot 2H_2O\}_n$ (Ln = Tb (1), Dy (2), and Yb (3)). In these complexes, the DTE ligand is in its open form with a parallel configuration and bridges lanthanide ions through its carboxylato groups. In this parallel configuration, the methyl groups of the two thiophene rings are on the same side of the perfluorocyclopentene, which blocks photo-isomerization to the closed form. The three chain complexes exhibited slow relaxation of the magnetization, which indicates that they have SMMs behavior.

2. Materials and Methods

The reagents and solvents were purchased from Tokyo Chemical Industry (Tokyo, Japan), Strem (Newburyport, MA, USA) or Wako Chemicals (Osaka, Japan) and were used without further purification. Elemental analyses for C, N, and H were performed with a Perkin-Elmer 240C elemental analyzer (PerkinElmer, Waltham, MA, USA) at the Research and Analytical Centre for Giant Molecules, Tohoku University. The ligand in its protonated form was synthesized by following a previously reported method [11].

Synthesis of Lanthanide Complexes. All of the complexes were synthesized by using a similar procedure. A typical procedure for 1 is described here. At room temperature and under aerobic condition, a methanol solution of $TbCl_3\cdot 6H_2O$ (21.2 mg, 0.046 mmol) and the DTE ligand (18.2 mg, 0.049 mmol) was stirred for 5 min and was layered on distilled water in test tube. Colorless crystals suitable for single crystal X-ray were obtained after 3–4 days. Elemental Analysis: for 1, Calculated ($C_{35}H_{22}F_{12}O_{10}S_4Tb$): C 38.23, H 1.83. Found: C 37.88, H 1.89; for 2, Calcd. ($C_{35}H_{22}F_{12}O_{10}S_4Dy$): C 38.07, H 1.92. Found: C 37.64, H 1.87; for 3, Calcd. ($C_{35}H_{22}F_{12}O_{10}S_4Yb$): C 37.74, H 1.81. Found: C 37.55, H 1.87.

X-ray Crystallographic Analyses. Single-crystal crystallographic data were collected on a Rigaku Saturn70 CCD diffractometer (Rigaku, Tokyo, Japan) with graphite-monochromated Mo $K\alpha$ radiation (λ = 0.71075 Å) produced using a VariMax micro-focus X-ray rotating anode source at 93 K. Single crystals with dimensions of 0.10 × 0.10 × 0.05 mm^3 for 1, 0.10 × 0.10 × 0.05 mm^3 for 2 and 0.10 × 0.05 × 0.03 mm^3 for 3 were used. Data processing was performed using the CrystalClear crystallographic software package [12]. The structures were solved by using direct methods via SIR-92 or SIR-2011 [13]. Refinement was carried out using WinGX 2013.3 packages [14] and SHELXL-2013 [15]. The non-H atoms were refined anisotropically using weighted full-matrix least squares on F^2. H atoms attached

to the C atoms were positioned using idealized geometries and refined using a riding model. Positions of the H atoms on the water molecules were determined using the CALC-OH software provided by WinGX [16]. CCDC-1452487-1452489 contains the supplementary crystallographic data for this paper. These data can be obtained free of charge from The Cambridge Crystallographic Data Centre.

Magnetism Studies. Magnetic susceptibility measurements were performed on polycrystalline samples on a Quantum Design MPMS-XL SQUID magnetometer (Quantum Design, San Diego, CA, USA). Experimental data were corrected for diamagnetism of the sample holder. The inherent diamagnetism of the materials was calculated and corrected by using Pascal's tables [17]. Ac measurements were performed in a 3 Oe oscillating magnetic field with and without a static dc field.

3. Results and Discussion

The three complexes crystallized in the monoclinic $C2/c$ space group. The crystallographic data are summarized in Table 1.

Table 1. Crystallographic data of Complexes.

Complex	1	2	3
Formula	$C_{35}H_{22}F_{12}O_{10}S_4Tb$	$C_{35}H_{22}F_{12}O_{10}S_4Dy$	$C_{35}H_{22}F_{12}O_{10}S_4Yb$
Mr/g mol^{-1}	1117.70	1121.27	1131.80
Crystal system	Monoclinic	Monoclinic	Monoclinic
Space group	$C2/c$	$C2/c$	$C2/c$
a/Å	35.9505(106)	35.8577(39)	36.0071(168)
b/Å	10.3997(30)	10.3531(8)	10.3359(46)
c/Å	10.4496(30)	10.4158(11)	10.3599(48)
β/°	95.9205(35)	96.0006(50)	95.5797(64)
V/Å^3	3886.0(2)	3845.6(5)	3837.3(3)
Z	4	4	4
T/K	93.15	93.15	96.15
Diffraction reflection	$4.118 \leqslant 2\theta \leqslant 27.576$	$4.099 \leqslant 2\theta \leqslant 27.523$	$4.005 \leqslant 2\theta \leqslant 27.431$
ρ_{calcd}/g cm^{-3}	1.910	1.937	1.959
μ/mm^{-1}	2.150	2.277	2.771
Number of reflections	7573	15193	7322
Independent reflections	4395	4439	4243
$F_0^2 > 2\sigma(F_0)^2$	3847	3941	2506
Number of variables	322	322	285
R_{int}, $R1$, $wR2$	0.0226, 0.0271, 0.0599	0.0321, 0.0252, 0.0544	0.0850, 0.0827, 0.2130

The three complexes are isostructural, and 1 will be described in detail as a reference. The [Tb(H-DTE)(DTE)(MeOH)· H_2O] unit is obtain by applying the $C2$ symmetry operation on the asymmetric unit (Figure 2 and Figure S1). This $C2$ axis is collinear with the Tb–O5 bond, creating a disorder of the MeOH and H_2O molecules (Figure S2). In the DTE ligand, the methyl groups adopt a parallel configuration with a C5–C13 distance of 4.202(4) Å, which is too long for photoisomerization of the ligand [7]. To satisfy the neutral nature of the complex, one proton is delocalized between the two O2 atoms of neighboring DTE ligands. Hydrogen bonds exist also between O2 and the water molecule. The coordination sphere of the Tb^{III} ion, composed of six oxygen atoms from DTE ligands and one oxygen atom from MeOH ligand (Figure S3), was determined to be a capped trigonal prism (Table S1). Each Tb^{III} ion are coordinated by six DTE ligands. One carboxylato group of a DTE ligand (O3, O4) bridge two Tb ions, and only O1 of the other carboxylate group of the DTE coordinates to a third ion. The coordination mode of the DTE ligand leads to an infinite 1D chain in the c direction (Figure S4). The Tb–Tb distance in the chain is 5.520 Å.

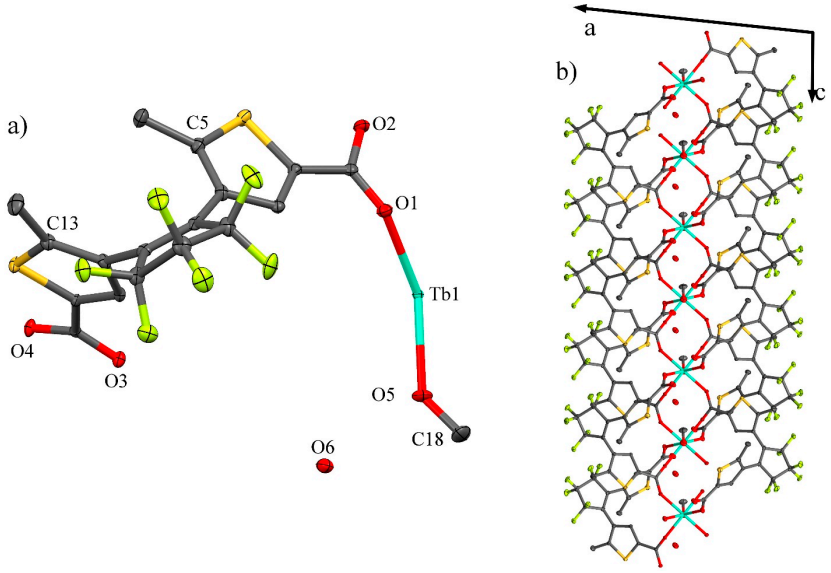

Figure 2. (**a**) *Oak Ridge Thermal Ellipsoid Plot* (ORTEP) view of the asymmetric unit of 1 with thermal ellipsoids drawn at 30% probability. H atoms are omitted for clarity. Tb, MeOH and H_2O have an occupancy of ½. (**b**) View of the 1D chain.

Magnetic Properties: The magnetic susceptibilities (χ) of the three complexes were measured between 300 and 2 K (Figure 3). At room temperature, χT value of 1 was 9.55 $cm^3 \cdot Kmol^{-1}$, significantly lower than the expected value of 11.82 $cm^3 \cdot Kmol^{-1}$ for a free Tb^{3+} ion [18]. This difference was attributed to non-population of some m_J level at energy not thermally available. Upon decreasing the temperature, depopulation of the m_J level occurred, and the susceptibility decreased continuously with an acceleration below 15 K, reaching a value of 5.35 $cm^3 \cdot Kmol^{-1}$ at 2 K. For complex 2, χT decreased from 15.07 $cm^3 \cdot Kmol^{-1}$ at room temperature to 11.49 $cm^3 \cdot Kmol^{-1}$ at 2 K. The value obtained at 300 K is higher than the expected one of 14.17 $cm^3 \cdot Kmol^{-1}$ for a free Dy^{3+} ion. This difference cannot be suitably explained. Complex 3 exhibited the same behavior with a χT of 2.41 $cm^3 \cdot Kmol^{-1}$ at 300 K consistent with the expected value for a free Yb^{III} ion (2.57 $cm^3 \cdot Kmol^{-1}$), which decreased to 0.92 $cm^3 \cdot Kmol^{-1}$ at 2 K.

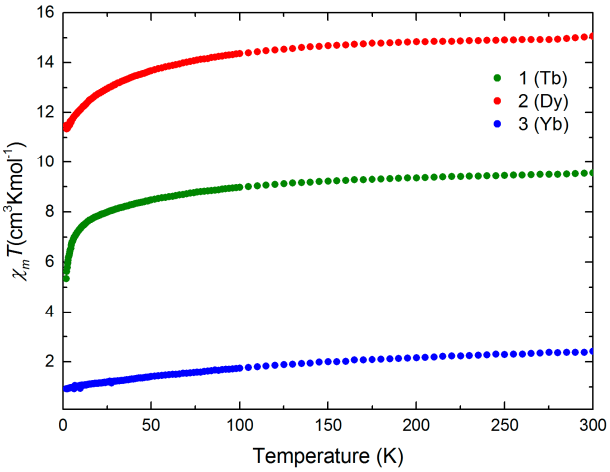

Figure 3. Temperature dependence of χT for poly-crystalline samples of complexes 1, 2 and 3.

The magnetization of 1 saturated at 3.67 Nβ in fields greater than 1.5 T, and that for 3 saturated at 2.34 Nβ over 4 T. In the case of 2, pseudo-saturation was observed over 2.5 T with a linear slope of 0.21 $N\beta T^{-1}$, and the magnetization was 5.51 Nβ at 5 T (Figure S5).

For all three complexes, no clear frequency dependence of χ was observed without an applied static magnetic field. In a dc field, a multi-peak signal was observed for each complexes with an optimum field of 5000 Oe for 1, 2500 Oe for 2, and 2000 Oe for 3 (Figure S6).

The frequency dependence of the in-phase (χ′) component and out-of-phase component (χ″) of the ac susceptibility in an optimized dc field at several *T* for each complex was analyzed using an extended Debye model [19] (Cf ESI for Equation S1) (Figure 4).

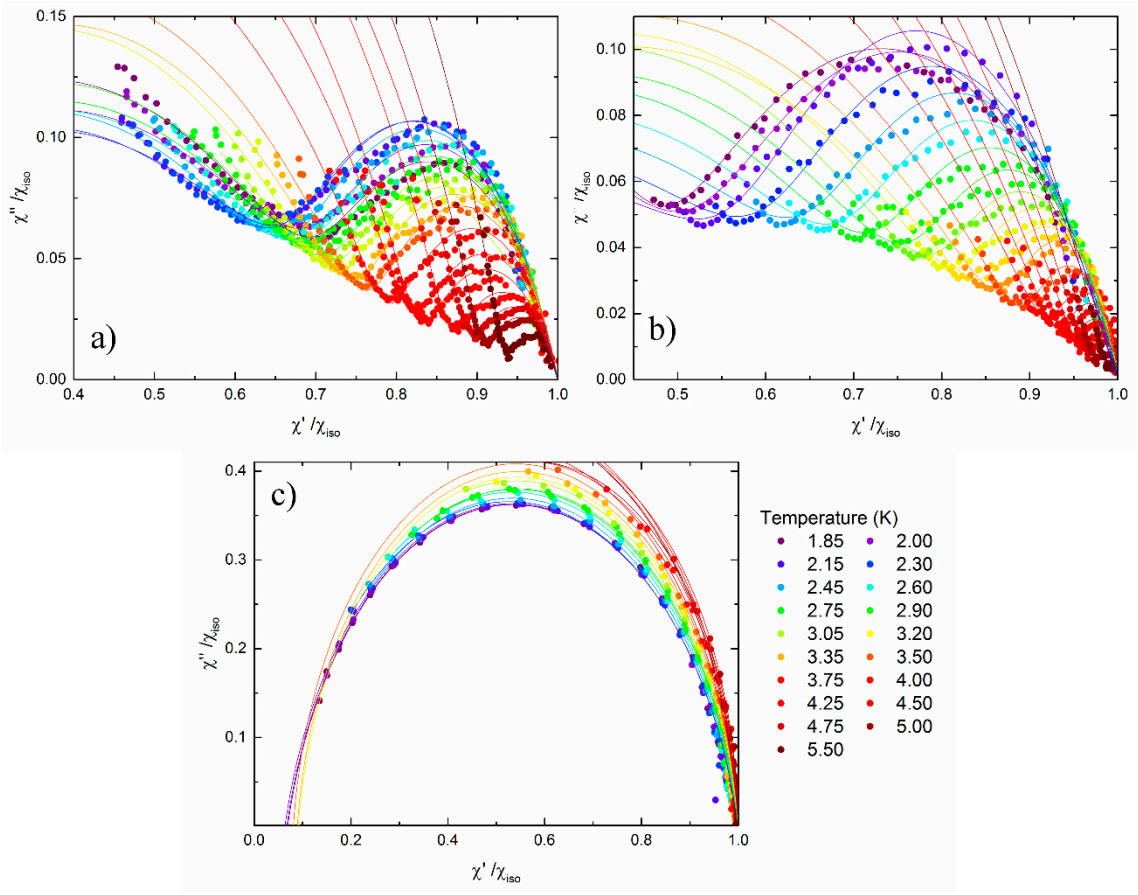

Figure 4. Normalized Argand plot for (**a**) 1 in a dc field of 5000 Oe; (**b**) 2 in a dc field of 2500 Oe and (**c**) 3 in a dc field of 2000 Oe. Point represent experimental data, and the lines were fitted to the data.

The presence of several relaxation times, especially in a short time range, makes it difficult to fit the experimental data with a physical meaning. For 3, a main relaxation time with a "tail" in the low frequency region was observed. We extracted the main relaxation process only (Figures 4c and 5, Tables S2 and S3), using Equations S2–S4 [20]. The relaxation time of 3 was fit as a function of *T* with a dc field of 2000 Oe, where A is the direct relaxation process parameter of 1.47×10^{-11} and τ_0 is the pre-exponential factor of 8.13×10^{-7} s, and the energy barrier for the reversal of the magnetization (Δ) was calculated to be 27 cm^{-1}. For 1 and 2, the calculations were more complicated. For these complexes, at least three relaxation peaks were visible: two weak peaks at low frequency and the main relaxation process over 1500 Hz.

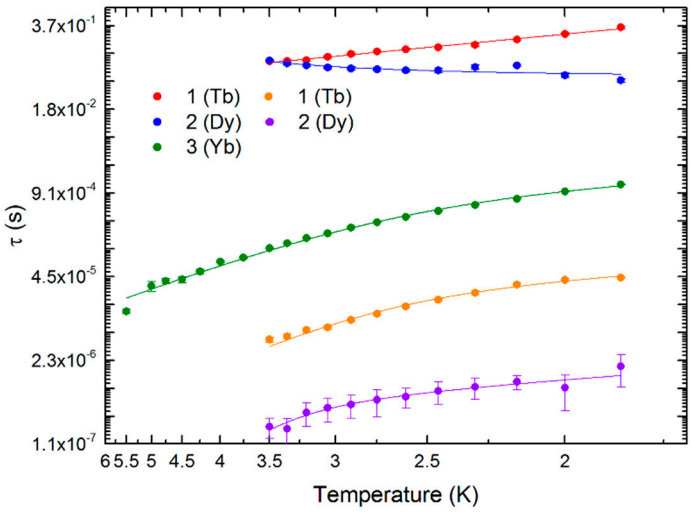

Figure 5. Relaxation time (τ) *vs. T* for the three complexes. The lines represent the best fits obtained by using Equation S5.

For 1, the two low frequency peaks were close together, appearing like a single asymmetric peak. Nevertheless, the difference was too small to be able to fit them independently. A dual relaxation time Debye model (one low and one high frequency) with the adiabatic χ (χ_{adia}) = 0 was used to determine the relaxation time (Figure 4a, Table S4). Under these conditions, the fast relaxation process mechanism was determined to be a combination of direct and Orbach relaxation processes with Δ = 33.3 cm^{-1} (Table S2). Complex 2 exhibited the same behavior as that of 1 with two close relaxation times at low frequency, which could not be fitted separately. Similar to the case of 1, a dual relaxation time Debye model with χ_{adia} = 0 was used to determine the relaxation times for 2 (Figure 4b, Table S5). Direct and Orbach processes with Δ = 59 cm^{-1} are dominant at high frequency (Table S2). In the low frequency region, the extracted relaxation time does not have a physical meaning since it increases with an increase in *T*. The results for 1 and 2 indicate that considering the two close relaxation processes as one broad peak is not suitable for analyzing the frequency dependence of χ as a function of *T*.

Moreover, the results can be discussed in the light of previous reports [21]. Complexes 1–3, which have three different lanthanide ions, are isostructural, but their SMM behaviors are different. 1 and 2 with Tb^{III} and Dy^{III} ions, respectively, show very short relaxation times, whereas 3 with Yb^{III} ions exhibits a moderate relaxation time. Tb^{III} and Dy^{III} ions have an oblate distribution of the 4f-shell electron which need an axial sandwich-type crystal field to minimizes the energy of the $m_J = J$ state, the preferential state to obtain SMMs. Yb^{III} ion have an prolate distribution of the 4f-shell electron, which need an equatorial crystal field to stabilize the $m_J = J$ state, and induce SMMs behavior. In the first approximation, it is easy to consider the coordination geometry and the crystal field to be same. The three complexes are isostructural and their coordination geometry is C2v, closer to being sandwich-type than it is to an equatorial one (Tables S1 and S6). However complex 3 exhibits better SMM behavior than 1 or 2. In fact, considering coordination geometry and crystal field as same is not a good approximation in our case. The field strength of the ligand plays a key role in the crystal field. In our complexes, three types of coordinating oxygen atoms are present: the neutral oxygen of the coordinated methanol (O5), the deprotonated bridging carboxylato group (O3, O4), and the protonated carboxylato group (O1). Considering the charge distribution around the lanthanide ions, the O3–O4–O3–O4 pseudo plan, the O1 and the O5 are charged −2, −½ and 0 respectively. In this configuration the crystal field become more equatorial than sandwich, and explain why the complex 3 show better SMM behavior than complexes 1 and 2.

4. Conclusions

Three isostructural SMMs with lanthanide ions and a DTE ligand were synthesized. In these complexes, the DTE ligand cannot photo-isomerize between the open and closed forms due to the parallel configuration of the methyl groups of the thiophene groups. The magnetization of the complexes did not show hysteresis, and the χ values were frequency independent without a static magnetic field. In optimal magnetic fields, the complexes underwent multiple relaxation processes. Only the Δ for the Yb^{III} complex could be determined. For the other two complexes with Tb^{III} and Dy^{III} ions, the relaxation time are out of the measurable range of our equipment or too close to be extracted with any physical meaning.

Supplementary Materials: The following are available online at www.mdpi.com/2312-7481/2/2/21/s1, Figure S1: Hydrogen bond between O6–O2 and O2–O2. Water and MeOH molecule have occupancy of 0.5; Figure S2: Disorder of MeOH and water molecule; Figure S3: Coordination polyhedron around the Tb ion; Figure S4: Crystal packing of Tb crystal in the *ab* plane; Figure S5: Magnetization curves of the three complexes at 1.82 K; Figure S6: Out-of-phase signal of ac susceptibility at 1.85 K in various fields (**a**, **c**, **e**), and at various temperature in optimum field (**b**, **d**, **f**), for complexes 1 (**a**, **b**), 2 (**c**, **d**) and 3 (**e**, **f**). The optimum field, defined as the field where the intensity of peak is maximized and the peak have lowest frequency, was determined to be 5000 Oe for 1, 2500 Oe for 2 and 2000 Oe for 3; Table S1: Determination of polyhedron geometry by using SHAPE 2.1 software; Table S2: Summary of the parameters used in Equations S1–S5 to fit τ; Table S3: Fitting parameters for complex 3; Table S4: Fitting parameters for complex 1; Table S5: Fitting parameters for complex 2. Table S6: Summary of some bonds length and distance in angstrom.

Author Contributions: M.A.Y. performed the experiments; G.C. conceived and designed the experiments; M.M. and M.I. synthesized the ligand; G.C. and B.K.B. wrote the paper; M.Y. supervised and managed the project.

Conflicts of Interest: The authors declare no conflict of interest.

References

1. Katoh, K.; Isshiki, H.; Komeda, T.; Yamashita, M. Molecular spintronics based on single-molecule magnets composed of multiple-decker phthalocyaninato terbium(III) complex. *Chem. Asian J.* **2012**, *7*, 1154–1169. [CrossRef] [PubMed]
2. Bogani, L.; Wernsdorfer, W. Molecular spintronics using single-molecule magnets. *Nat. Mater.* **2008**, *7*, 179–186. [CrossRef] [PubMed]
3. Mills, D.P.; Moro, F.; McMaster, J.; van Slageren, J.; Lewis, W.; Blake, A.J.; Liddle, S.T. A delocalized arene-bridged diuranium single-molecule magnet. *Nat. Chem.* **2011**, *3*, 454–460. [CrossRef] [PubMed]
4. Gatteschi, D.; Sessoli, R. Quantum tunneling of magnetization and related phenomena in molecular materials. *Angew. Chem. Int. Ed.* **2003**, *42*, 268–297. [CrossRef] [PubMed]
5. Leuenberger, M.N.; Loss, D. Quantum computing in molecular magnets. *Nature* **2001**, *410*, 789–793. [CrossRef] [PubMed]
6. Liddle, S.T.; van Slageren, J. Improving f-element single molecule magnets. *Chem. Soc. Rev.* **2015**, *44*, 6655–6669. [CrossRef] [PubMed]
7. Sorace, L.; Wernsdorfer, W.; Thirion, C.; Barra, A.-L.; Pacchioni, M.; Mailly, D.; Barbara, B. Photon-assisted tunneling in a Fe_8 single-molecule magnet. *Phys. Rev.* **2003**, *68*. [CrossRef]
8. Inose, T.; Tanaka, D.; Tanaka, H.; Ivasenko, O.; Nagata, T.; Ohta, Y.; de Feyter, S.; Ishikawa, N.; Ogawa, T. Switching of single-molecule magnetic properties of Tb^{III}–porphyrin double-decker complexes and observation of their supramolecular structures on a carbon surface. *Chem. Eur. J.* **2014**, *20*, 11362–11369. [CrossRef] [PubMed]
9. Pinkowicz, D.; Ren, M.; Zheng, L.-M.; Sato, S.; Hasegawa, M.; Morimoto, M.; Irie, M.; Breedlove, B.K.; Cosquer, G.; Katoh, K.; *et al*. Control of the single-molecule magnet behavior of lanthanide-diarylethene photochromic assemblies by irradiation with light. *Chem. Eur. J.* **2014**, *20*, 12502–12513. [CrossRef] [PubMed]
10. Irie, M. Diarylethenes for memories and switches. *Chem. Rev.* **2000**, *100*, 1685–1716. [CrossRef] [PubMed]
11. Morimoto, M.; Irie, M. Photochromic reactions of diarylethenes in single crystals with intermolecular O–H$\cdots$N hydrogen-bonding networks. *Chem. Eur. J.* **2006**, *12*, 4275–4282. [CrossRef] [PubMed]
12. CrystalClear-SM, 1.4.0 SP1; Rigaku Corporation: Tokyo, Japan, 17 April 2008.

13. Altomare, A.; Burla, M.C.; Camalli, M.; Cascarano, G.L.; Giacovazzo, C.; Guagliardi, A.; Moliterni, A.G.G.; Polidori, G.; Spagna, R. SIR97: A new tool for crystal structure determination and refinement. *J. Appl. Crystallogr.* **1999**, *32*, 115–119. [CrossRef]
14. Farrugia, L.J. WinGX and ORTEP for Windows: An update. *J. Appl. Crystallogr.* **2012**, *45*, 849–854. [CrossRef]
15. Sheldrick, G.M. Crystal structure refinement with SHELXL. *Acta Cryst. C* **2015**, *71*, 3–8. [CrossRef] [PubMed]
16. Nardelli, M. Modeling hydroxyl and water H atoms. *J. Appl. Crystallogr.* **1999**, *32*, 563–571. [CrossRef]
17. Bain, G.A.; Berry, J.F. Diamagnetic corrections and Pascal's constants. *J. Chem. Educ.* **2008**, *85*. [CrossRef]
18. Kahn, O. *Molecular Magnetism*; VCH Publishers: Weinheim, Germany, 1993.
19. Katoh, K.; Horii, Y.; Yasuda, N.; Wernsdorfer, W.; Toriumi, K.; Breedlove, B.K.; Yamashita, M. Multiple-decker phthalocyaninato dinuclear lanthanoid(III) single-molecule magnets with dual-magnetic relaxation processes. *Dalton Trans.* **2012**, *41*, 13582–13600. [CrossRef] [PubMed]
20. Pedersen, K.S.; Ungur, L.; Sigrist, M.; Sundt, A.; Schau-Magnussen, M.; Vieru, V.; Mutka, H.; Rols, S.; Weihe, H.; Waldmann, O.; *et al*. Modifying the properties of 4f single-ion magnets by peripheral ligand functionalisation. *Chem. Sci.* **2014**, *5*, 1650–1660. [CrossRef]
21. Rinehart, J.D.; Long, J.R. Exploiting single-ion anisotropy in the design of f-element single-molecule magnets. *Chem. Sci.* **2011**, *2*, 2078–2085. [CrossRef]